EB2023-CMT-001

Influence of carbide feedstock on properties of protective laser claddings for grey cast iron brake rotors

Andreas Wank [1*], Christian Schmengler [1], Diana Pehl [1], Annika Krause [1], Sascha Barteck [1]

[1] *GTV Verschleiss-Schutz GmbH, Vor der Neuwiese 7, 57629 Luckenbach, Germany (E-Mail: a.wank@gtv-mbh.de)*

DOI (FISITA USE ONLY)

ABSTRACT: Laser cladding is frequently applied for development of wear and corrosion protective coatings on grey cast iron brake rotors. Stainless steels are cost effective materials but achieve only poor wear resistance without hard phase reinforcement. Fused tungsten carbide is a frequently applied hard phase. However, it easily dissolves in stainless steel melt forming brittle mixed carbides. NbC and TiC show better metallurgical compatibility because they re-precipitate without formation of brittle phases. While TiC reinforcement results in slightly higher crack formation tendency, NbC shows disadvantages concerning pricing and availability of raw material. Besides leached NbC cubes, sintered and crushed pure TiC and NbC, plasma spheroidized pure TiC, agglomerated and sintered as well as sintered and crushed TiC/FeCr and NbC/FeCr composite powders are applied for production of reinforced stainless steel coatings on grey cast iron brake rotors. The powders are evaluated concerning their impact on feed rate stability, on dissolution and embedding in the stainless steel matrix and on strength of the produced claddings. The irregular shape of sintered and crushed powders results in feed rate stability restrictions and relatively strong dissolution in the steel matrix melt. Cracks formed during the crushing procedure are not completely penetrated by steel matrix melt. Plasma spheroidization of TiC powder permits achieving high feed rate stability and avoiding presence of cracks in carbide particles. Spray dried and sintered TiC/FeCr composite powder permits excellent feed rate stability and low dissolution in the steel matrix melt. However, large particles that are not fully penetrated by steel matrix melt show only low cohesive strength and can cause microcrater formation during grinding of claddings. Sintered and crushed TiC/FeCr composite powder shows good feed rate stability, low dissolution in the steel matrix melt and high cohesive strength within composite particles.

KEY WORDS: laser cladding, TiC, NbC, fused tungsten carbide, cermet

1. INTRODUCTION

Recent development of wear and corrosion protective surfaces for grey cast iron brake rotor friction ring surfaces focusses on high velocity oxygen fuel (HVOF) or cold gas sprayed coatings and laser claddings [1]. While HVOF and cold gas sprayed coatings can provide advantageous compressive residual stress state and permit up to 80 vol.% hard phase content in protective coatings, laser claddings feature metallurgical bonding to substrates and gas tightness. Excellent deposition efficiency of 90% at deposition rates of up to 16 kg/h makes laser cladding processes economically interesting [2]. With the aim not only to minimize overall fine dust emission but also to exclude release of hazardous debris from brake disk claddings typically carbide reinforced stainless steels are applied. There is a wide spectrum of potentially suitable carbide feedstock powders for production of reinforced stainless steel claddings. These powders are manufactured by various production methods and show different chemical composition, particle size distribution, particle shape, morphology, and carbide size [3].

Carbides differ concerning their general metallurgical compatibility with stainless steel matrices. Silicon carbide shows particularly fast dissolution in iron based matrix melt resulting in formation of brittle phases and formation of crack networks [4]. Also, relatively weak carbide forming elements like chromium, molybdenum and tungsten will form mixed carbides after dissolution in iron based melts, which limits the process parameter range for cladding production significantly [5]. Contrary, titanium and niobium are strong carbide formers, and their carbides will re-precipitate as mono carbides without formation of brittle mixed carbides from iron based melts.

Besides commercially available spherical fused tungsten carbide (FTC_s) various niobium and titanium carbide powders have been used in combination with different stainless steel matrix materials to clad grey cast iron brake rotors evaluating their aptitude for use as reinforcing phase in protective claddings. The investigations cover sintered and crushed pure titanium and niobium carbide powders as well as niobium carbide cubes produced by leaching. Also, effect of post treatment by plasma spheroidizing has been studied at the example of sintered and crushed titanium carbide. Furthermore, composite powders consisting of titanium or niobium carbides with an average size of roughly 1 µm and FeCr matrices have been produced by spray drying and sintering as well as sintering and crushing.

2. Experimental

All tests have been carried out using a high power diode laser LDF 22000-100 source (Laserline GmbH, Mülheim-Kärlich, D) along with quasi-coaxial six-stream powder nozzles type GTV PN6625 (GTV Verschleiss-Schutz GmbH, D). Laser beam (4.9 mm diameter) and powder streams are focused on workpiece surfaces in the powder nozzle´s nominal working distance of 25 mm. Precise adjustment of powder particle density distribution and particle speed is secured by use of individual powder feed lines connected to each powder injection port with mass flow control of carrier gas and closed-loop control of powder feed rate in g/min. Ranges of applied process parameters for coating of vented grey cast iron brake rotors (figure 1) are listed in table 1. Friction ring surfaces are prepared by dry turning prior to cladding.

Figure 1 Vented grey cast iron brake rotor with protective laser cladding on friction ring surface

Table 1 Applied process parameter ranges

Laser power [kW]	16.0 - 22.0
Welding speed [m/s]	1.0 - 6.7
Powder feed rate [g/s]	1.7 - 5.0
Overlap [%]	85 - 97
Nozzle gas Ar [nlpm]	30 - 50
Carrier gas Ar [nlpm]	15 - 24
Carbide content [wt.%]	< 50%
Layer thickness [µm]	80 - 400

Powders and coating cross sections are analyzed by optical and scanning electron microscopy as well as HV0.3 microhardness measurements.

3. RESULTS

3.1. Spherical fused tungsten carbide powder

Spherical fused tungsten carbide powder showing a nominal size fraction of +20 -53 µm (d_{50} ~ 40 µm in Cilas 920 laser scattering analyses) is applied for reinforcement of stainless steel matrices. Maximum achievable hard phase content in claddings without crack formation depends on several factors. Generally, residual stresses rise with increasing friction ring surface area and cladding thickness. Deposition of buffer layers without hard phase reinforcement and pre-heating are effective measures to reduce residual stresses and thereby permit production of layers with high hard phase content avoiding crack formation. For example, crack formation can be avoided for cladding of 300 µm AISI 316L - 30 wt.% FTCs layers on 120 µm AISI 316L buffer layers without pre-heating (figure 2, bottom), but direct deposition on grey cast iron substrates will result in crack formation. 120 µm AISI 316L buffer layers and pre-heating to 350 °C permit up to 45 wt.% FTC$_s$ reinforcement without crack formation.

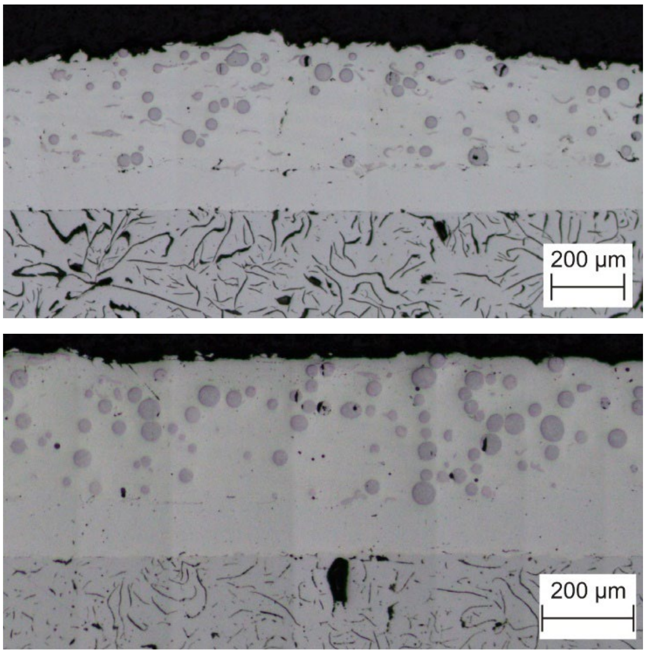

Figure 2 Optical micrographs of laser claddings with top layers consisting of AISI 316L - 30 wt.% FTC$_s$
laser power 21 kW, powder feed rate 3.8 g/s, welding speed 2.5 m/s, carrier gas flow rate for steel powder 4x 3 nlpm, carrier gas flow rate for FTC$_s$ powder 2x 4 nlpm (top) / 2x 6 nlpm (bottom)

FTC$_s$ particle speed is a function of powder nozzle bore diameter and carrier gas flow rate and takes strong influence on the morphology and phase composition of claddings. With increasing carrier gas flow rate particle speed increases and heat transfer from the laser beam to inflight particles decreases. If carrier gas flow rate is low, especially small particles can melt on their way through the laser beam and get embedded as flat lamellae inside the cladding microstructure or even get dissolved in the steel melt (figure 1, top). Dissolution of tungsten and carbon results in formation of brittle mixed carbides and finally crack formation. Using excessive carrier gas flow rate causes rebounding of a large share of FTC$_s$ from the workpiece surface. Adequate carrier gas flow rates permit embedding of FTC$_s$ particles with only minimal dissolution in the stainless steel matrix (figure 1, bottom). In such case microhardness testing shows an extremely wide range of individual microhardness HV0.3 values, i.e., from 400 to 2500 HV0.3. Even average values of 10 measurements can differ from 900 to 1400 HV0.3.

Dendrites of tungsten rich mixed carbides are formed in the vicinity of FTC$_s$ particles that have been heated up excessively on their way into the melt pool (figure 3) resulting in embrittlement.

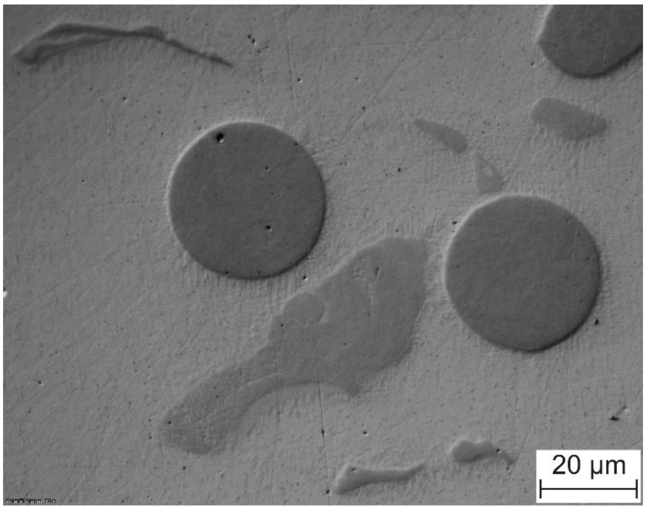

Figure 3 High resolution optical micrograph of an AISI 316L - 30 wt.% FTC_s laser cladding produced with 2x 4 nlpm carrier gas flow rate for FTC_s powder

3.2. Leached pure niobium carbide powder

Cubic pure niobium carbide particles with a nominal size fraction of +10 -53 µm (d_{50} ~ 30 µm in Cilas 920 laser scattering analyses) can be produced by leaching of the metallic matrix from a cast niobium and carbon rich iron based alloy block (figure 4). Such powder shows good flow characteristics and permits high feed rate stability.

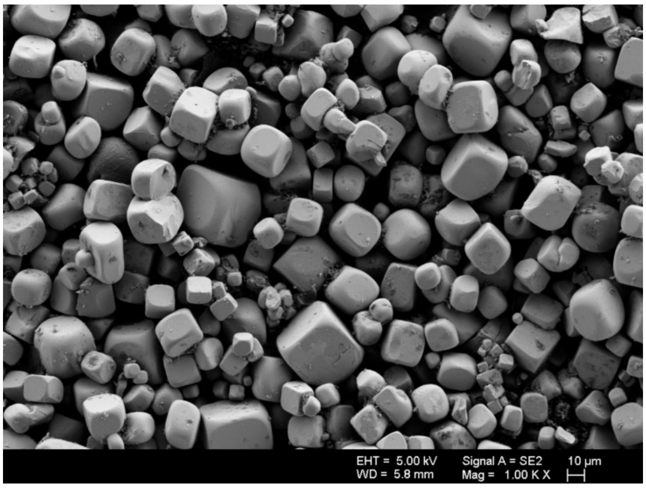

Figure 4 Scanning electron micrograph of a leached pure niobium carbide cube powder

There is good wetting of the NbC cubes by the stainless steel matrix melt. Due to the relatively small specific surface area of the cubes only little dissolution and re-precipitation of niobium carbides occurs (figure 5). The precipitates show submicron size and round shape. No pre-heating is needed to realize 30 vol.% reinforcement of an AISI 318LN steel matrix without crack formation. However, there is alumina contamination of the cubic NbC powder due to the leaching of the iron based matrix that contains aluminum. Alumina strongly absorbs laser radiation resulting in its evaporation and finally formation of craters as deep as the deposited layer thickness [2]. Therefore and because of a maximum annual availability of only a few tons leached carbide feedstock has been discarded.

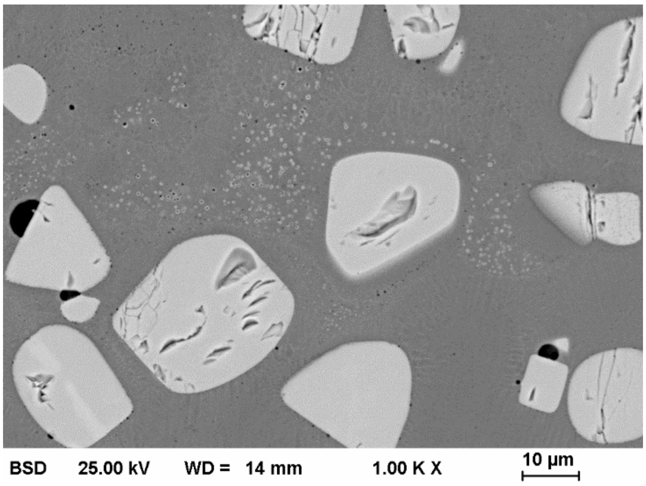

Figure 5 Scanning electron micrograph of an AISI 318LN - 30 wt.% NbC laser cladding produced with cubic NbC particles

3.3. Sintered and crushed pure carbide powders

Sintered and crushed pure niobium and titanium carbide powders are commercially available from various suppliers. Due to the irregular particle shape (figure 6) acceptable powder feed rate stability can only be achieved if the content of fines in the particle size distribution is strictly limited. Powder with a nominal size fraction of +10 -53 µm (d_{50} ~ 40 µm in Cilas 920 laser scattering analyses) has proven to permit stable feeding conditions. Generally, also coarser powder can be applied. However, likeliness that particles are not incorporated into the coating microstructure and coating roughness increase with particle size.

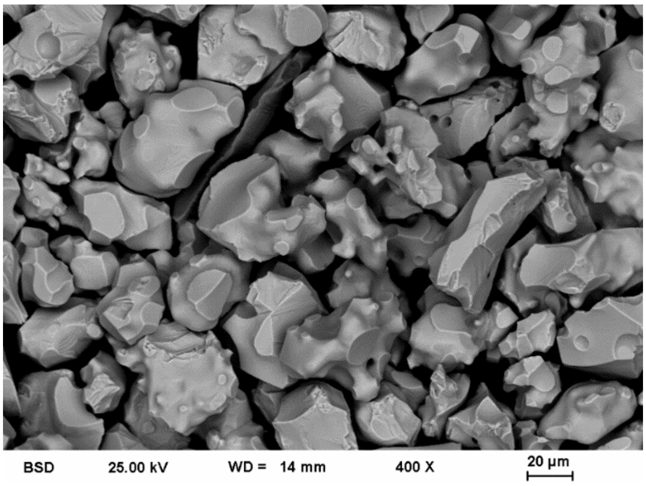

Figure 6 Scanning electron micrograph of a sintered and crushed pure niobium carbide powder

Good wetting of both sintered and crushed TiC and NbC powders by various stainless steel matrix melts is observed. However, the particle´s large specific surface area causes relatively strong dissolution. High contents of carbon and titanium / niobium in the vicinity of carbide particles results in formation of dendritic carbides, while precipitates in areas with lower contents of carbon and titanium / niobium show round shape and submicron size (figure 7). Stainless steel melt penetrates open pores during cladding formation, while remaining closed porosity after sintering is transferred into the cladding microstructure. Relatively large carbide particles can break during grinding leaving cracks with a length exceeding 20 µm already in as ground claddings (figure 7). Also, cracks propagate much faster in brittle carbides than in ductile stainless steel matrix. On the other hand, large hard phase contact area might be advantageous with respect to wear under tribological load.

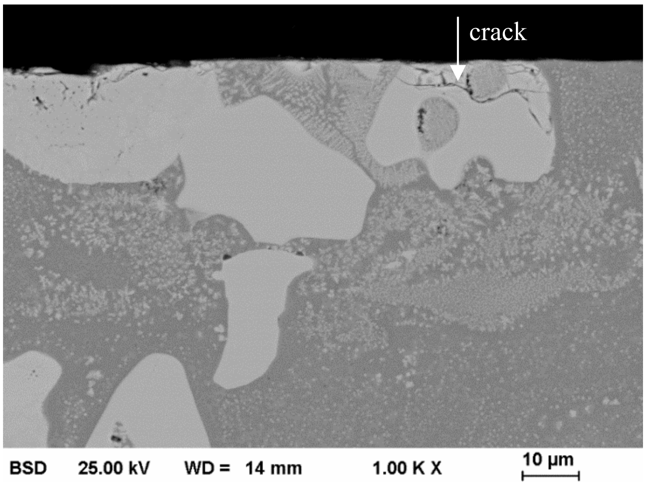

Figure 7 Scanning electron micrograph of an AISI 318LN - 30 wt.% NbC laser cladding produced with sintered and crushed pure NbC powder

3.4. Spray dried and sintered composite powders

High sphericity composite powders consisting of micron sized TiC (figure 8) or NbC particles (each FSSS ~ 1 µm) and stainless chromium steel matrices with a volumetric matrix fraction of roughly 20%, i.e., NbC-20wt.%FeCr and TiC-30wt.%FeCr, are produced by spray drying and sintering. NbC/FeCr and TiC/FeCr powders show nominal size fractions of +15 -38 µm and +10 -53 µm (d_{50} ~ 25 µm and ~ 35 µm in Cilas 920 laser scattering analyses) respectively. Spherical particle shape results in excellent flow characteristics and feed rate stability.

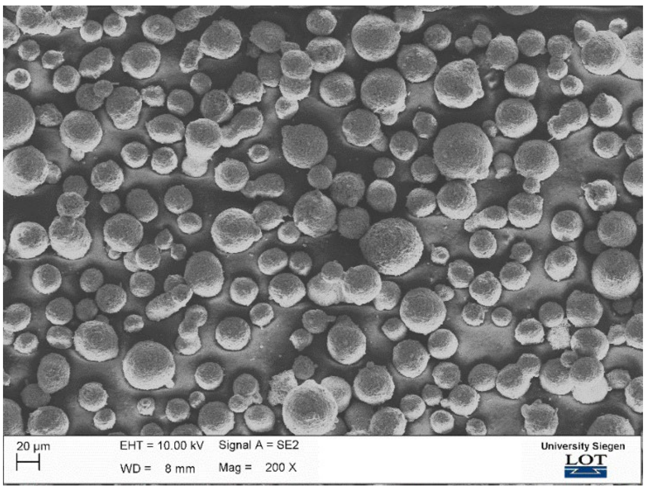

Figure 8 Scanning electron micrograph of a spray dried and sintered TiC/FeCr 70/30 powder

Wetting of the composite particles by the stainless steel matrix melt is excellent. The very small specific surface area results in only little dissolution and re-precipitation of round submicron sized carbides, but some composite particles break up and the contained primary carbides get dispersed in the stainless steel matrix (figure 9). Even without pre-heating 30 vol.% carbide reinforcement of various stainless steel matrices does not result in crack formation. Such coatings show only small differences of local microhardness HV0.3 (standard deviation < 100 HV0.3) and average values between 500 to 700 HV0.3.

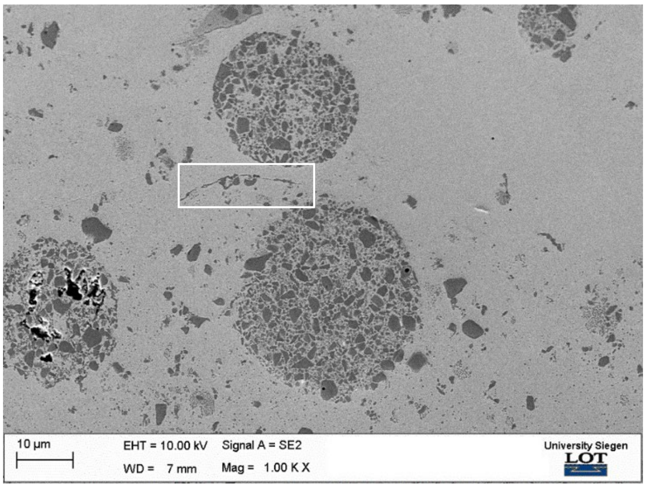

Figure 9 Scanning electron micrograph of an AISI 316L laser cladding reinforced with 24 wt.% spray dried and sintered TiC/FeCr 70/30 composite powder; the highlighted rectangular area marks a band of re-precipitated TiC

Microstructure of claddings with NbC/FeCr and TiC/FeCr reinforcement is almost the same. However, formation of bands of re-precipitated carbides (figure 9) is only observed for use of TiC based composites. Spray dried and sintered composite particles are porous. Stainless steel matrix melt penetrates most of those pores. However, high welding speeds cause rapid solidification and especially for large composite particles penetration of pores is sometimes not completed (figure 9). There is a relatively high chance that material breaks out from incompletely penetrated composite particles during grinding procedures leaving microcraters behind (figure 10). Also, the relatively weak cohesion inside incompletely penetrated composite particles can cause break out of material due to tribological load during braking resulting in formation of small scratches in circumferential direction.

3.5. Sintered and crushed composite powders

Sintered and crushed composite powders consisting of micron sized TiC (figure 11) or NbC particles (each FSSS ~1 µm) and stainless chromium steel matrices are produced with the same carbide content as spray dried and sintered composite powders, i.e., NbC-20wt.%FeCr and TiC-30wt.%FeCr. Due to their irregular shape a sufficiently coarse nominal size fraction of +15 -63 µm (d_{50} ~ 40 µm in Cilas 920 laser scattering analyses) needs to be applied to achieve good feed rate stability.

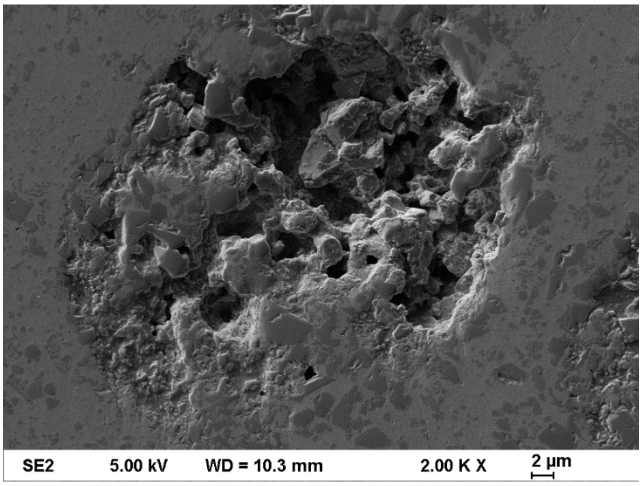

Figure 10 Scanning electron micrograph of an incompletely penetrated TiC/FeCr 70/30 composite particle causing formation of a microcrater during grinding

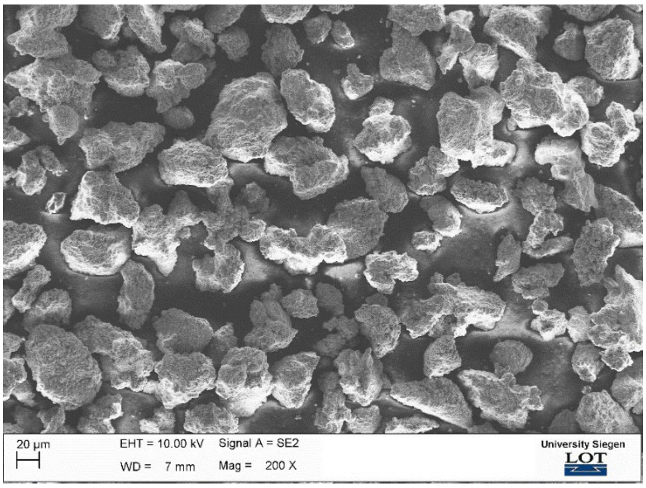

Figure 11 Scanning electron micrograph of a sintered and crushed TiC/FeCr 70/30 powder

Excellent wetting of the composite particles by the stainless steel matrix melt is observed. Despite the relatively large specific surface area only little dissolution and re-precipitation of round submicron sized carbides occurs. However, many fine composite particles break up and the contained primary carbides are dispersed in the stainless steel matrix (figure 12).

Like for use of spray dried and sintered composites various stainless steel matrices can be reinforced with up to 30 vol.% carbide crack free without pre-heating and average coating microhardness between 500 to 700 HV0.3 is achieved. Also, formation of bands of re-precipitated carbides (figure 12) is only observed for use of TiC based composites. Some small, closed pores remaining after the sintering process are transferred into the cladding microstructure. However, the composites show strong cohesion and therefore break-out of material during grinding procedure or due to tribological load during braking is securely avoided.

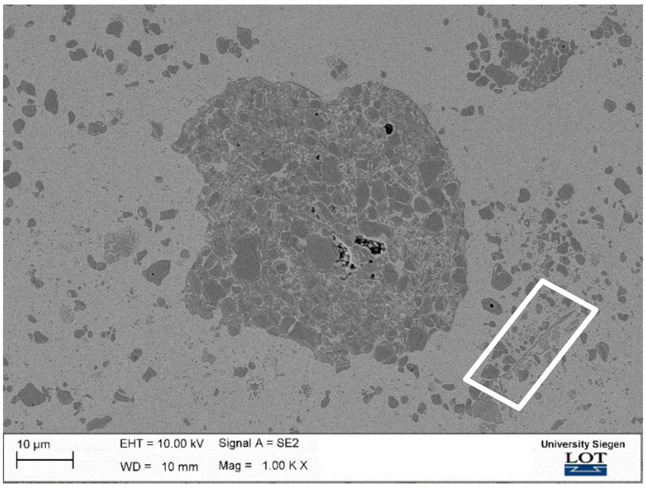

Figure 12 Scanning electron micrograph of an AISI 316L laser cladding reinforced with 24 wt.% sintered and crushed TiC/FeCr 70/30 composite powder; the highlighted area marks a band of re-precipitated TiC

3.6. Plasma spheroidized pure TiC powder

Plasma spheroidizing tests with sintered and crushed pure TiC described in chapter 3.3 resulted in formation of high sphericity TiC particles only for a maximum diameter of roughly 30 µm (figure 13). Larger particles have not been melted and mostly maintained their irregular shape. In Cilas 920 laser scattering analyses $d_{50} \sim 40$ µm is determined. Sphere shape especially of fine particles results in excellent flow characteristics and feed rate stability.

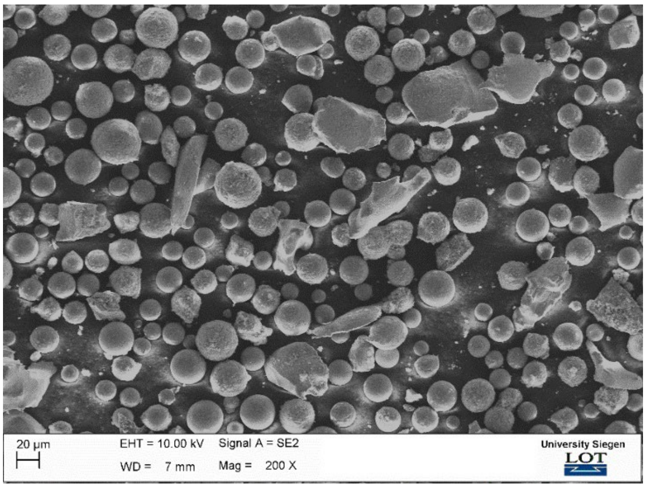

Figure 13 Scanning electron micrograph of a plasma spheroidized pure TiC powder

Like for all other TiC based powders excellent wetting by the stainless steel matrix melt is observed. Due to the strongly reduced specific surface area compared to sintered and crushed pure TiC powder only very little dissolution and re-precipitation of round submicron sized TiC is observed (figure 14). Crack free AISI 316L stainless steel claddings with 30 vol.% carbide reinforcement can be produced without pre-heating. Plasma spheroidizing improves strength of TiC particles significantly. Contrary to sintered and crushed pure TiC powder grinding results in only negligible crack formation in plasma spheroidized TiC particles.

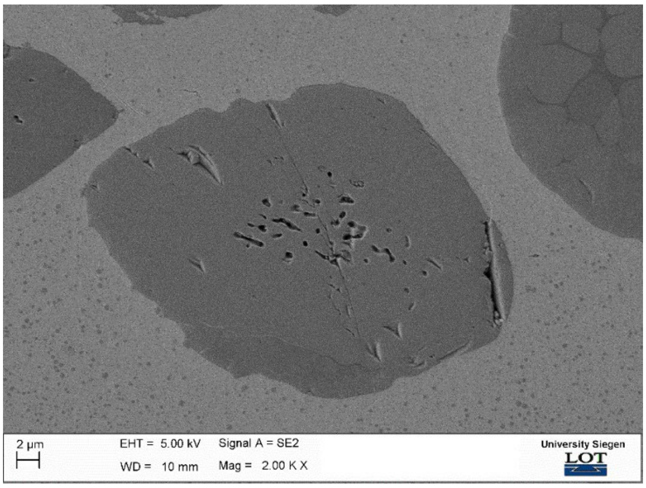

Figure 14 Scanning electron micrograph of an AISI 316L laser cladding reinforced with 24 wt.% plasma spheroidized pure TiC powder

Plasma spheroidizing represents an expensive additional process step in powder production. For processing of TiC particles larger than 30 µm suitable parameters need to be developed and the capacity of readily installed systems is not adequate for mass production of brake disks with protective laser claddings.

4. DISCUSSION

There is a wide spectrum of carbides that are generally suitable for manufacturing of reinforced stainless steel claddings to protect grey cast iron brake disk friction ring surfaces against wear and corrosion. Use of carbides from strong carbide forming elements results in improved process robustness, because dissolution in stainless steel melt does not result in formation of brittle mixed carbides. It is possible to produce high quality protective claddings using fused tungsten carbide powder for reinforcement. However, the applicable range of process conditions is very narrow. Limiting of heat transfer to inflight carbide particles is crucial. Therefore, it is advisable to feed fused tungsten carbide powder separately to permit independent adjustment of their speed on the way from the powder nozzle into the melt pool on the workpiece.

TiC and NbC do not form brittle mixed carbides after dissolution in stainless steel melts and therefore permit robust production of protective claddings. However, feed rate stability, interaction of carbide particles with the stainless steel melt and crack formation tendency vary strongly depending on the applied production method. Table 2 contains a comprehensive evaluation of various feedstock production routes.

Cubic carbide powder produced by leaching is not applicable unless oxide contamination will be excluded. Also, availability is very poor. Contrary, sintered and crushed pure carbide powders as well as spray dried and sintered or sintered and crushed composite powders show good availability and producers are ready to expand production capacity as needed. Sintered and crushed pure carbide powders require relatively large particle size to avoid feed rate instabilities resulting in low crack resistance during grinding and relatively strong dilution due to large specific surface area impairs cladding strength. Post-treatment by plasma spheroidizing is effective to improve feed stability and reduce dilution in stainless steel matrix melts strongly. However, the additional process is costly and there is only very small free capacity on existing installations.

Table 2 Comprehensive evaluation of TiC and NbC based powder feedstock production routes with respect to manufacturing of protective laser claddings on grey cast iron brake disks

production route	feed stability	dilution in matrix	carbide crack resistance	cladding strength	availability
leaching	+	+	+	+	--
sintering and crushing	-	-	-	0	+(+)
plasma spheroidizing	++	+	+	+	-
spray drying and sintering, composite	++	+	++	0	+(+)
sintering and crushing, composite	+	+	++	+	+(+)

+ positive, - negative

Small carbide size in composite powders secures excellent crack resistance of the contained carbides. While spray dried and sintered powders show excellent feed stability, their low cohesion requires full penetration of pores by stainless steel melt to avoid formation of microcraters during grinding or braking. Sintered and crushed composite powders show advantageous resistance against formation of such microcraters and represent the best possible compromise for TiC and NbC based feedstock for reinforcement of stainless steel matrices.

While TiC shows cost advantages compared to NbC, no formation of carbide bands is observed for use of NbC resulting in a slightly improved resistance against crack formation and propagation in respective claddings.

4. SUMMARY AND CONCLUSIONS

In contrast to fused tungsten carbide niobium and titanium carbide do not form brittle mixed carbides after dissolution in stainless steel melt. Therefore, they permit production of crack free protective claddings on grey cast iron brake rotors in a wider range of process parameters. Among the tested hard phases niobium and titanium carbides with an average size of only ~1 µm embedded in an iron based alloy matrix show the highest crack resistance. Contrary to sintered and crushed TiC/FeCr and NbC/FeCr composite powders, porous agglomerated and sintered composite powders require full penetration by steel matrix melt to avoid presence of weak spots that can cause formation of microcraters during grinding procedures. As niobium carbide does not form carbide bands like titanium carbide, it permits achieving the highest resistance against crack formation and propagation in carbide reinforced stainless steel claddings.

REFERENCES

[1] Vasiljević, S., J. Glišović, B. Stojanović, A. Vencl: Review of the coatings used for brake discs regarding their wear resistance and environmental effect. Proc. Inst. Mech. Eng., Part J: J. Eng. Tribol. 236 (2022) 10, 1932-1949. doi:10.1177/13506501211070654

[2] Wank, A., C. Schmengler, A. Krause, K. Müller-Roden, T. Wessler: Environmentally Friendly Protective Coatings for Brake Disks. J. Therm. Spray Technol. 32 (2023) 2-3, 443-455. https://doi.org/10.1007/s11666-022-01459-0

[3] Fauchais, P., G. Montavon, G. Bertrand: From Powders to Thermally Sprayed Coatings. J. Therm. Spray Technol. 19 (2010) 1-2, 56-80. https://doi.org/10.1007/s11666-009-9435-x

[4] Rettig, M., J. Grochowicz, K. Käsgen, R. Eaton, A. Wank, A. Hitzek, C. Schmengler, S. Koss, M. Voshage, J.H. Schleifenbaum, C. Verpoort, T. Weber: Carbidic Brake Rotor Surface Coating Applied by High-Performance Laser-Cladding. Proc. EuroBrake 2020, EB2020-MDS-025, 1-8. https://doi.org/10.46720/eb2020-mds-025

[5] Hofer, B.: Heiß-Isostatisches-Pressen (HIP) Anwendungen in der Kunststoffmaschinenindustrie, Proc. SKZ Conference Verschleiß und Verschleißschutz an Kunststoffverarbeitungsmaschinen, slide 31, in German.